

Quantitative Determination of Quantum Fluctuations in the Spin-1/2 Planar Antiferromagnet

R. R. P. Singh, P. A. Fleury, K. B. Lyons, and P. E. Sulewski

AT&T Bell Laboratories, Murray Hill, New Jersey 07974

(Received 13 March 1989; revised manuscript received 11 April 1989)

Frequency moments of the light-scattering spectrum from spin-pair excitations are calculated for the spin- $\frac{1}{2}$ planar Heisenberg antiferromagnet. The quantitative agreement with the experimental B_{1g} spectrum in La_2CuO_4 demonstrates that the observed linewidth is dominated by quantum fluctuations and yields a value for the exchange parameter J of $1030 \pm 50 \text{ cm}^{-1}$. Quantum fluctuations also permit light scattering due to diagonal-next-neighbor spin-pair excitations. Observed spectral features in the A_{1g} and B_{2g} symmetries are consistent with those calculated for this process.

PACS numbers: 75.40.Gb, 75.30.Ds, 75.50.Ee

The effects of quantum fluctuations on the static and dynamic properties of two-dimensional spin- $\frac{1}{2}$ quantum antiferromagnets have been the subject of numerous theoretical studies¹ over the past thirty years. Quantum corrections, for example, to the sublattice magnetization, M^+ , the spin-wave velocity, C_s , and the perpendicular susceptibility, χ_\perp , for the nearest-neighbor square lattice Heisenberg antiferromagnet were originally studied via a $1/S$ expansion in the spin-wave theory.² In contrast to these expansions, which are asymptotic, convergent expansions have now been developed for these quantities by perturbing around the Ising limit.³ These latter expansions open up the possibility of *directly* computing the experimentally observable static and dynamic properties of Heisenberg antiferromagnets in a controlled and systematic manner.

The quantum corrections are expressed most appropriately⁴ in terms of multiplicative renormalizations of the classical values. For example, the spin-wave velocity becomes $C_s = Z_c \sqrt{8SJ}a/\hbar$, where J is the exchange constant for the Heisenberg Hamiltonian and the classical value of C_s for $S = \frac{1}{2}$ is $\sqrt{2}Ja/\hbar$. In most experiments the renormalization parameter (such as Z_c) is not independently determined, so that the role of quantum fluctuations, embodied in Z , is not directly tested.

In this Letter we show that the light-scattering spectrum from spin-pair excitations in La_2CuO_4 provides dramatic evidence for the role of quantum fluctuations in these systems as well as a quantitative determination of the microscopic exchange parameter. The Ising expansions³ are used to estimate the various frequency moments of the spectrum (for B_{1g} symmetry) for comparison with those observed experimentally. The predicted first moment can be used to deduce the exchange parameter J , while the ratios of the higher moments to the first one, or the ratio of the peak width to its position, provide a quantitative, parameter-free check on the theoretical prediction for the effect of quantum fluctuations. We find that the agreement between the theory and the experiments is excellent. This demonstrates clearly that the observed B_{1g} peak width is intrinsic to the $S = \frac{1}{2}$

Heisenberg system. Furthermore, the ratio of the peak width to its position differs from the purely classical prediction⁵ by a factor of 3, thus highlighting the role of quantum fluctuations.

In addition we show that light scattering from diagonal-next-neighbor spin-pair excitations, forbidden in the classical limit, is permitted by quantum fluctuations. The calculated spectral moments and the relative spectral weights of these features are both in fairly good agreement with recently observed A_{1g} and B_{2g} peaks in La_2CuO_4 .

We begin with the antiferromagnetic (AFM) Hamiltonian

$$H = J_z \sum_{\langle ij \rangle} S_i^z S_j^z + J_{xy} \sum_{\langle ij \rangle} (S_i^x S_j^x + S_i^y S_j^y), \quad (1)$$

where the Heisenberg model corresponds to $J_{xy} = J_z = J$. Following Ref. 3, we expand quantities of interest in powers of x ($= J_{xy}/J_z$) and extrapolate the series to estimate them for the Heisenberg model ($x=1$). The scattering Hamiltonian describing the interaction of the spin pairs with photon pairs (for B_{1g} symmetry) is given by⁵

$$H_R = \sum_{\langle ij \rangle} (\mathbf{E}_{\text{inc}} \cdot \boldsymbol{\sigma}_{ij}) (\mathbf{E}_{\text{sc}} \cdot \boldsymbol{\sigma}_{ij}) \mathbf{S}_i \cdot \mathbf{S}_j, \quad (2)$$

where \mathbf{E}_{inc} and \mathbf{E}_{sc} are the electric field vectors for the incident and scattered photons, and $\boldsymbol{\sigma}_{ij}$ is a unit vector connecting spin sites i and j . We first restrict our attention to the case where i and j are nearest neighbors only, which gives rise to B_{1g} scattering only. The symmetry notation used throughout is appropriate to the tetragonal, D_{4h} , structure. At the end of this paper we will briefly discuss the consequences of adding a diagonal-next-neighbor term to Eq. (2).

The scattered spectrum, at $T=0$, is given by

$$I(\omega) = \sum_i \delta(\omega - (E_i - E_0)) |\langle 0 | H_R | i \rangle|^2, \quad (3)$$

where E_i is the i th eigenenergy of (1) and $|0\rangle$ is the ground state. The spectral moments ρ_n are simply obtained in terms of multiple-spin correlations in the

ground state of (1). In particular,

$$\begin{aligned}
 I_T &= \int I(\omega) d\omega = \langle 0 | H_R^2 | 0 \rangle, \\
 \rho_1 &= \int \omega I(\omega) d\omega / I_T = \langle 0 | H_R [H, H_R] | 0 \rangle / I_T, \\
 \rho_2 &= \int \omega^2 I(\omega) d\omega / I_T = -\langle 0 | [H, H_R]^2 | 0 \rangle / I_T, \\
 \rho_3 &= \int \omega^3 I(\omega) d\omega / I_T = \langle 0 | [H, [H, H_R]] [H, H_R] | 0 \rangle / I_T, \\
 &\text{etc.}
 \end{aligned}
 \tag{4}$$

$$\begin{aligned}
 \rho_1/J &= 3 + 0x + \frac{1}{2}x^2 + 0x^3 + 0.0286x^4 + 0.0372x^5 + 0.0159x^6 + \dots, \\
 \rho_2/J^2 &= 9 + 0x + \frac{10}{3}x^2 + 0x^3 + 0.719x^4 + 0.290x^5 + 0.0828x^6 + \dots, \\
 \rho_3/J^3 &= 27 + 0x + 17.16x^2 + 0x^3 + 6.474x^4 + 1.663x^5 + 0.711x^6 + \dots.
 \end{aligned}
 \tag{5}$$

In order to facilitate the comparison with experiments, we consider the cumulants

$$(M_n)^n = \int (\omega - \rho_1)^n I(\omega) d\omega / I_T, \tag{6}$$

for $n > 1$, and $M_1 = \rho_1$.

Since the light scattering is dominated by short-wavelength (or zone boundary) excitations, the singularity in these series caused by the long-wavelength spin waves (Goldstone modes) is expected to be extremely weak. Hence it is appropriate to extrapolate these series using ordinary Padé approximants. Using these extrapolations we obtain $\rho_1/J = 3.58 \pm 0.06$, $M_2/J = 0.81 \pm 0.05$, and $M_3/J = 1.00 \pm 0.14$, where the uncertainties reflect the spread in the Padé approximants.

The light-scattering experiments were carried out on single crystals of La_2CuO_4 obtained from two sources using two different preparative methods. The experimental details have been published elsewhere,⁷ as has the dependence of experimental scattering efficiency upon laser excitation wavelength (between 6328 and 4579 Å).

As shown in Fig. 1(a), the B_{1g} spectral feature is peaked near 3200 cm^{-1} , is reasonably symmetric near the peak, and exhibits nonzero intensity out to 7000 cm^{-1} . The scattering geometries and selection rules were as previously described,^{7,8} with the axes x and y along the Cu-O bond direction and x' , y' at 45° . We note that $x'x'$ corresponds to $A_{1g} + B_{2g}$, xy to B_{2g} , and $x'y'$ to B_{1g} . Thus A_{1g} is given by $x'x' - xy$. To minimize laser heating or photodecomposition of the samples, the incident beam ($< 20\text{-mW}$ total power) was focused to a line of $\sim 100\text{-}\mu\text{m}$ width by 1.5-mm length.

Results from two samples of La_2CuO_4 are presented below. Neither crystal has been subjected to post-growth annealing procedures. The first was grown in PbO-CuO flux, and contains $\sim 1\%$ Pb as a substitutional impurity, with basal-plane dimensions $8 \times 10 \text{ mm}^2$. The other crystal was grown (at higher temperature) from pure CuO flux and thus contains no major impurities.

Although Eq. (4) is valid, strictly speaking, only for $T=0$, we expect it to hold for $T \ll J$. Indeed, no appreciable temperature variation is observed in La_2CuO_4 for $0 < T < 300 \text{ K}$.

The reason for calculating the moments rather than the full line shape is apparent from Eq. (4). The moments are properties of the ground state; hence, the resulting expansions will be convergent for all values of $x \leq 1$. In contrast, the excited states entering Eq. (3) may encounter several singularities (or level crossings) as x is varied between 0 and 1. The series are developed by the method of Singh, Gelfand, and Huse.⁶ We obtain

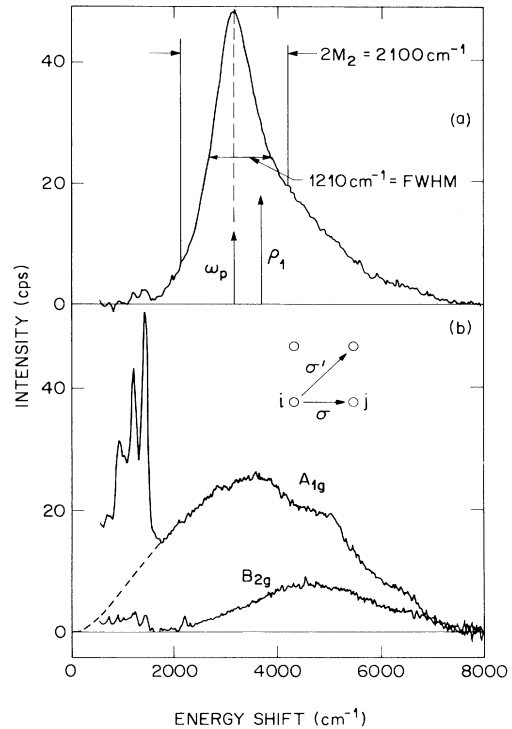


FIG. 1. All spectra were excited with 4880-Å light and fully corrected for all instrumental response. (a) Comparison of $B_{1g}(x'y')$ spin-pair spectrum in La_2CuO_4 with various calculated moments. The peak frequency, ω_p , is seen to be slightly smaller than the first moment or the "central" frequency ρ_1 . The second cumulant, M_2 , measures the width of the peak. The observed ratio M_2/ρ_1 is in good agreement with the calculated value of 0.23. (b) $A_{1g}(x'x' - xy)$ and $B_{2g}(xy)$ spectra from the same sample. The experimental moments are as follows, $\rho_1 \approx 3700 \text{ cm}^{-1}$ and $M_2 \approx 1400 \text{ cm}^{-1}$ excluding the phonon contributions as shown by the dashed line; B_{2g} , $\rho_1 \approx 4500 \text{ cm}^{-1}$ and $M_2 \approx 1200 \text{ cm}^{-1}$. The ratio of B_{2g} to A_{1g} integrated intensities is ≈ 0.25 .

TABLE I. Experimental values for the peak frequency and first, second, and third cumulants of the B_{1g} in two samples of La_2CuO_4 for various laser excitation wavelengths.

Sample	λ_L (Å)	ω_p (cm^{-1})	M_1 (cm^{-1})	M_2 (cm^{-1})	M_3 (cm^{-1})	M_2/M_1
$\text{La}_2\text{CuO}_4:\text{Pb}$	5145	3170	3350 ± 50	950 ± 100	700 ± 200	0.28
	4880	3170	3680	1000	900	0.27
	4579	3155	3725	1180	1100	0.32
La_2CuO_4	5145	3260	3740	920	900	0.25
	4880 ^a	3170	3700	1050	1000	0.28
	4579	3180	3740	1130	1100	0.30
Theory			$(3.6 \pm 0.1)J$	$(0.8 \pm 0.1)J$	$(1.0 \pm 0.2)J$	0.23

^aSpectrum displayed in Fig. 1(a).

This crystal has a measured antiferromagnetic transition temperature of 265 K. Scattering spectra were obtained from the (001) crystal faces. The B_{1g} spectrum from the Pb-free sample is displayed in Fig. 1(a). To gain an appreciation of the influence of errors in the background subtraction procedure, as well as the possible influence of resonant enhancements in the scattering cross section to the observed line shapes, we have collected in Table I the experimental values of ρ_1 , M_2 , M_3 , and the peak position ω_p for a variety of incident laser wavelengths for both types of samples.

Extraction of a value for J from these spectra requires a model for the spin-fluctuation dynamics. Spin-wave theory has been used previously.⁵ This approach works well for $S=1$. In our original report,⁸ we noted that spin-wave theory predicts a peak at $\omega_p \cong 2.7J'$, realizing that J' must be corrected for quantum effects in the case of $S = \frac{1}{2}$. Our experiment emphasizes short-range fluctuations (or large- k zone-boundary spin waves). Assuming that the spin-wave spectrum is renormalized from its classical form by a single k -independent renormalization $Z = 1.18 \pm 0.02$,³ this yields $J = 1000 \text{ cm}^{-1}$. Recent inelastic neutron scattering⁹ in La_2CuO_4 has directly resolved the long-wavelength spin-wave dynamics, yielding a spin-wave velocity of $0.85 \pm 0.3 \text{ eV \AA}$. Using the same Z , this leads to $J = 1080 \pm 40 \text{ cm}^{-1}$.

We now compare these results of spin-wave theory with the present theory, which explicitly includes quantum fluctuations. Although the present theory predicts a very different peak shape, the value extracted for J is hardly changed. From Eq. (5) and Table I, we can obtain the microscopic exchange, J , from the experimental first moment ρ_1^{expt} . This value, $J = 1030 + 50 \text{ cm}^{-1}$, is to be compared with any microscopic calculation for J . Several have appeared. Some¹⁰ are clearly better than others.¹¹

The shape of the spectrum provides a stringent test of the applicability of this calculation. Equations (5) and (6) provide direct theoretical values for the frequency moments of the spectrum; hence we can obtain a

parameter-free test of the theory. For example, the predicted ratio M_2/M_1 relates the spin-pair linewidth to the central frequency in terms which are independent of J . This ratio differs from a classical calculation⁵ by a factor greater than 2, thus demonstrating the dominant role of quantum fluctuations in the linewidth. Furthermore, the ratio M_3/M_1 is a prediction for the skewness of the intensity pattern and helps to put bounds on the high-frequency tails of the spectrum.

As can be seen by comparing Table I to the calculated cumulants given after Eq. (6), the agreement between theory and experiment is very good. The experimental and theoretical values for M_2/M_1 are 0.27 ± 0.03 and 0.23 ± 0.02 , respectively, and the experimental and theoretical values for M_3/M_1 are 0.27 and 0.27, respectively. The indicated experimental uncertainties arise mainly from uncertainties in subtraction of background fluorescence.¹²

We note that the theoretical calculation includes contributions to the spin-pair excitations from four magnons, six magnons, etc., because the ground state obtained by series expansion has components with a large number of spins flipped with respect to the classical (Néel) ground state. Figure 1(a) exhibits appreciable scattering intensity above $4J$ (the classical spin-pair cutoff frequency). Thus, one simple reason why the classical calculation gives a much narrower spectrum than is observed is that it entirely ignores the higher magnon contributions. We note further that the agreement between theory and experiment for the third cumulant within errors shows that there is no appreciable scattering beyond the experimental range shown in Fig. 1 ($\sim 8000 \text{ cm}^{-1}$).

Finally, we turn briefly to the A_{1g} and B_{2g} spectral features shown in Fig. 1(b). The A_{1g} feature and its resonance behavior were first reported in Ref. 7, which suggested that it might arise from either higher-order spin excitations or coupled charge and spin excitations. Here we present arguments that this scattering originates from diagonal-next-neighbor (DNN) spin-pair excitations

which are Raman active solely by virtue of quantum fluctuations.¹³ Adding such a DNN term to Eq. (2), replacing σ by σ' as in Fig. 1(b), makes no contribution to the B_{1g} spectrum, but gives rise to scattering in both the A_{1g} and B_{2g} geometries. Series expansions for the moments of these spectra carried out to order x^4 yield the following results: For A_{1g} , $M_1 \approx 3.5J$ and $M_2 \approx 1.2J$; for B_{2g} , $M_1 \approx 3.9J$ and $M_2 \approx 1.1J$. The ratio of the B_{2g} to A_{1g} integrated intensities [$R = I_T(B_{2g})/I_T(A_{1g})$] is predicted to be ~ 0.4 . These expectations are borne out by our experiments. Using the value of J determined from the B_{1g} spectrum, the values of M_1/J and M_2/J provide additional parameter-free predictions for comparison with the spectra in Fig. 1(b). All of these predictions agree with experiment to within $\sim 20\%$. The experimental value of R depends on laser wavelength, probably due to resonance effects and lies in the range 0.1–0.4.

Although this agreement strongly supports the identification of the Fig. 1(b) spectra as quantum-fluctuation-induced DNN spin-pair scattering, it is not fully conclusive. First, the uncertainties in these theoretical calculations are greater than for the B_{1g} case because the former have been carried out only to order x^4 . Second, unlike the B_{1g} spectra, both the A_{1g} and the B_{2g} exhibit significant ($\sim 25\%$) resonance effects in their overall line shapes. Third, absent a detailed calculation of the resonant enhancements for all three scattering geometries, we are unable to utilize the observed intensities of A_{1g} or B_{2g} , relative to B_{1g} , to rule out the participation of other (e.g., charge transfer) excitations⁷ in the spectra of Fig. 1(b). Clearly, more extensive theoretical and experimental work is needed to explicate fully the role of resonant enhancement in light scattering from the planar copper oxides.

In summary, we have presented here theoretical evaluations of the frequency moments for the light-scattering spectra from planar spin- $\frac{1}{2}$ Heisenberg antiferromagnets. For the B_{1g} spectrum these are in quantitative agreement with experiments in La_2CuO_4 and show that the observed linewidth is intrinsic and is caused by large quantum fluctuations in the $S = \frac{1}{2}$ system. The calculations also enable us to determine the microscopic exchange constant J , which is found to be $1030 \pm 50 \text{ cm}^{-1}$. Both the A_{1g} and B_{2g} spectra are in reasonable agreement with the relative intensities and the frequency moments calculated for scattering from DNN spin-pair excitations, whose Raman activity arises solely from quantum fluctuations.

The suggestion for the moment calculations came originally from Steve Girvin. We are grateful to David Huse, Peter Littlewood, and Sriram Shastry for helpful discussions. We thank A. S. Cooper, G. P. Espinosa, and Z. Fisk for the samples used in this study and in Ref. 7.

Note added.— We have now completed convergent expansion calculations to order x^2 for the more difficult $S=1$ case. The first and second moments agree with both the experiments and the spin-wave theory cited in Ref. 5.

¹F. Keffer, in *Encyclopedia of Physics*, edited by H. P. J. Wijn (Springer-Verlag, Berlin, 1966), Vol. XVIII.

²P. W. Anderson, *Phys. Rev.* **86**, 694 (1952); R. Kubo, *Phys. Rev.* **87**, 568 (1952); T. Oguchi, *Phys. Rev.* **117**, 117 (1960).

³R. R. P. Singh, *Phys. Rev. B* **39**, 9760 (1989).

⁴S. Chakarvarty, B. I. Halperin, and D. R. Nelson, *Phys. Rev. Lett.* **60**, 1057 (1988).

⁵J. B. Parkinson, *J. Phys. C* **2**, 2012 (1969). The classical theory discussed here was shown to be in essentially perfect agreement with light-scattering experiments in the $S=1$ case (K_2NiF_4) reported by P. A. Fleury and H. J. Guggenheim, *Phys. Rev. Lett.* **24**, 1346 (1970). By “classical” we mean that the ground state is assumed to be the Néel state.

⁶R. R. P. Singh, M. P. Gelfand, and D. A. Huse, *Phys. Rev. Lett.* **61**, 2484 (1988).

⁷K. B. Lyons *et al.*, *Phys. Rev. B* **39**, 9693 (1989). Substantial resonance enhancements have been reported earlier for both spin and phonon excitations by several groups. W. H. Weber *et al.*, *Phys. Rev. B* **38**, 917 (1988); S. Sugai *et al.*, *Jpn. J. Appl. Phys. Lett.* **26**, L495 (1987); S. Sugai *et al.*, *Phys. Rev. B* **38**, 6436 (1988).

⁸K. B. Lyons, P. A. Fleury, J. P. Remeika, A. S. Cooper, and T. J. Negran, *Phys. Rev. B* **37**, 2353 (1988).

⁹G. Aeppli *et al.* (to be published).

¹⁰M. S. Hybertsen, M. Schlüter, and N. E. Christensen, *Phys. Rev. B* **39**, 9028 (1989).

¹¹Y. Guo, J. M. Langlois, and W. A. Goddard, *Science* **239**, 896 (1988).

¹²A constant fluorescence background has been subtracted to obtain the B_{1g} and B_{2g} displayed in Fig. 1 and used for calculation of experimental moments. Spectra obtained using different laser excitation wavelengths indicate that the resulting B_{2g} spectrum of Fig. 1(b) contains little fluorescence.

¹³Although the exchange energy for the DNN will be much smaller than J in the unperturbed system, it is plausible that resonant enhancement effects in the optically perturbed system render the scattering intensities for the DNN and NN pair excitations comparable.